Wireless Netw (2016) 22:223–234
DOI 10.1007/s11276-015-0969-1

CrossMark

PN code acquisition using smart antennas and adaptive thresholding for spread spectrum communications

Aghus Sofwan[1] · Mourad Barkat[2] · Salman A. AlQahtani[1]

Published online: 20 May 2015

Abstract In this paper, we consider a pseudo-noise (PN) code acquisition for direct sequence spread spectrum communication in a Rayleigh fading multipath channel environment using smart antenna and adaptive thresholding automatic trimmed-mean constant false alarm rate (ATM-CFAR) processing. A smart antenna is an array of antenna elements that can modify the array pattern adaptively to minimize the effect of multiple access interference (MAI) from other users and multipath. PN code acquisition using a fixed threshold may lead to an excessive number of false alarms, and thus, adaptive thresholding ATM-CFAR processing is considered. In addition, since the interference (MAI and multipath) can be considered as outliers, an outlier determiner is embedded to the proposed system based on the interquartile range. This novel approach of combining smart antennas and adaptive thresholding ATM-CFAR detection with an outlier determiner proved to be very robust since it resulted in a serious enhancement of the probability of detection.

Keywords Automatic TM-CFAR · Interquartile range · LMS smart antenna · Outliers · PN code acquisition

✉ Salman A. AlQahtani
salmanq@ksu.edu.sa

Aghus Sofwan
aghus@yahoo.com

Mourad Barkat
mbarkat581@gmail.com

1 Department of Computer Engineering, College of Computer and Information Sciences, King Saud University, Riyadh, KSA

2 Department of Electrical and Computer Engineering Technology, Valencia College, Orlando, FL, USA

1 Introduction

Pseudo-noise (PN) code synchronization is an important stage in direct sequence spread spectrum (DS-SS) communication. There are two phases of code synchronization: code acquisition and code tracking. Code acquisition is the coarse alignment between the incoming PN code signal and the local dispreading code at the receiver. When the codes are aligned then this process yields a correlation value. Obtaining a high correlation value leads to a better detection for acquisition. The receiver multiplies both codes and the result is integrated over some observation interval. The multiplication and integration are performed one by one for each code phase to be examined. The code tracking is a finer alignment for synchronization between the transmitter and the receiver.

In code division multiple access (CDMA) communication systems, the presence of multiple access interference (MAI) is a major challenge that significantly affects the performance. Smart antenna applications are deployed more and more in mobile communication systems because of their benefits in providing more promising results such as combating MAI and reducing multipath fading [1]. Smart antennas can solve the limited bandwidth problems, follow many beams to track several mobiles, and improve the received signal power gain and thus increase the detection probability. Therefore, a combination of smart antenna and PN code acquisition technique is considered in mobile communication. There are many well-known adaptive algorithms to adjust the required weighting in a smart antenna such as least mean square (LMS), sample matrix inversion (SMI), and recursive least square (RLS) [2]. Smart antennas for PN code acquisition have also been considered. In [3], Bing and Kwon proposed a system utilizing the LMS algorithm with smart antennas and a fixed threshold for wireless communication while in [4] they consider smart antennas for PN code acquisition in direct sequence (DS) CDMA.

As mentioned previously, in order to decide to whether tracking or phase updating, the system uses a threshold value. If the threshold value is too high the probability of miss is increased, on the other hand, if the threshold is too low this may lead to a serious increase in the false alarm probability. Therefore, due to variations in the received signal power caused by the environmental influence and mobility, adaptive thresholding techniques based on maintaining the constant false alarm rate (CFAR), where the threshold value is set in accordance with the magnitude of background noise level, are preferred. Adaptive thresholding CFAR detection is well developed in automatic radar signal detection applications [5] and have also been applied in some CDMA communication applications.

In communication systems, the received signal contains noise and interfering signals that may be considered as outliers. The system must be able detect and trim the outliers to avoid unnecessary false alarms. In this paper, we identify the outlier by using the boxplot technique. The boxplot can give some information about the data set such as dispersion and identify outliers. The technique defines a resistant rule which is multiplication of a multiplier value ρ and dispersion for constructing fences. The data values exceeding the fences are defined as outliers.

In this paper, we consider PN code acquisition using smart antennas and adaptive thresholding ATM-CFAR processing with an outlier determiner for spread spectrum communication systems. The proposed PN code acquisition system uses smart antennas which would yield an increase in the signal to noise ratio (SNR) level and a serious interference reduction. We explore appropriate multiplier values of resistant rules to define demarcation points of outliers in the system. This novel combination of smart antenna and adaptive thresholding ATM-CFAR processing with an outlier determiner proved to be robust since it resulted in a significant enhancement of the detection probability as will be shown in the next sections.

The structure of this paper is as follows. In Sect. 2, we exhibit the related works on this area that have been conducted. In Sect. 3, we describe the proposed communication system model under consideration and present the problem formulation. We also obtain the conditional probability density functions under both hypotheses H_1 and H_0. In addition, we apply the first and the third quartiles to obtain a multiplier value ρ in order to identify the fences as demarcation points for the outliers. In Sect. 4, we compare the performance of the proposed system using adaptive cell averaging (CA)-CFAR processing to the system given in [3] which, recall, does not consider multipath. However, in the problem under consideration in this paper we do consider the presence of multipath and MAI, and also suggest the use of ATM-CFAR processing, which is based on rank order statistics in order to censor the cells containing interfering signals. Part of this paper was presented in [6], which considered the trimmed mean CFAR processing only instead of automatic censoring scheme using the outlier determiner. We investigate performance of the proposed system while reducing the effect of MAI and multipath. We also explore the multiplier value ρ to determine the fences for censoring the outlier cells in the reference cells. Furthermore, we derive an exact expression for the probability of detection and show the robustness of the system performance in terms of the theoretical probability of detection. The conclusion is given in Sect. 5.

2 Related work

In PN code acquisition techniques, several schemes have been proposed in the literatures, such as serial search acquisition [7, 8], parallel acquisition [9, 10], and hybrid acquisition [11, 12]. Antenna diversity has been proposed to further improve PN code acquisition such as decreasing the acquisition time and providing robustness in fading environments [13, 14]. The presence of MAI substantially affects the performance of CDMA communication systems. Various schemes have been proposed in the literature to suppress MAI [15–18]. In [15], multiuser interference cancellation in CDMA communication systems with diversity gain was introduced. Dodd et al. [16] proposed an iterative joint detection for MAI using DS-CDMA. In [17], a parallel interference cancellation using a combination of different linear equalization and a rake receiver was proposed for downlink CDMA systems. In Zhang et al. [18] proposed a multiuser detection system using smart antennas in a CDMA system to combat MAI in a multipath fading channel. Employing smart antenna to combat MAI in wireless communication systems was also considered in [19]. Smart antenna applications are continuously deployed in mobile communication systems because of their benefits. Recently, an implementation of the LMS and RLS algorithms with smart antennas to optimize the performance of advanced communication system was presented in [20].

Adaptive thresholding CFAR detection is well developed in automatic radar signal detection applications [5]. From the rich literature on CFAR detection, we cite some references from radar applications based on CA-CFAR in [21, 22] and robust order statistics (OS) CFAR processing in [23–25]. Adaptive thresholding techniques have also been applied in some CDMA communication applications. Several PN code acquisition schemes using adaptive thresholding CFAR processing have been addressed in [26–29] which show the enhancement of the detection probability. Just very recently, Berbra et al. [30] proposed an adaptive array acquisition system, which integrates an adaptive thresholding technique based on ordered data variability index constant false alarm rate (ODV-CFAR) and LMS algorithm for CDMA communication.

We cite literatures in detecting the outliers. In [31], forward methods were proposed in CA-CFAR processing for locating the outlier. Tuckey [32] developed the boxplot technique to determine possible outliers. Moreover, several techniques exploring data based on the boxplot resistant rules are given in [33–35].

3 System description and problem formulation

The communication system model considered assumes D users from simultaneous transmitters while the first user is considered as the initial synchronization whose performance is to be investigated. Figure 1 shows the block diagram of the proposed communication system model. The transmitted signal of the i-th user is given by

$$s_i(t) = \sqrt{2P_{T_i}} b_i(t) c_i(t) cos(\omega_c t + \xi_i) \tag{1}$$

where P_{T_i} is the transmitted power of the i-th signal, b_i is the data waveform, c_i is the spreading sequence, ω_c is the angular carrier frequency, and ξ_i is the phase of the i-th modulator from the transmitter. At the beginning of each transmission, the transmitter sends a phase coded carrier without data modulation to help the initial synchronization [7, 8]. Hence, we assume for simplicity that there is no data modulation on the initial synchronization signals.

The user signals are transmitted through a communication channel assumed to be a Rayleigh fading multipath channel. The transmitted signals are received by an antenna array of M elements and go through an LMS processor. The output from the LMS processor undergoes ATM-CFAR processing in order to make a final decision about acquisition or not.

3.1 The received signal model

The communication channel model considered consists of L tapped delay lines with a tap spacing of one chip [36] that correspond to the number of resolvable multipath with amplitudes α_{il} and phases ζ_{il}, $i = 1,\ldots, D$, $l = 0,\ldots, L-1$, where α_{il} is Rayleigh random variable and ζ_{il} is uniform random variable over $[0, 2\pi]$. We assume that the fading amplitude is constant during an observation interval but changes from one to another. Moreover, we normalize the total fading power in all resolvable paths to unity. The average fading power in each path is defined as [37]

$$E\left[\alpha_{il}^2\right] = \frac{1-\exp(-\mu)}{1-\exp(-\mu L)}\exp(-l\mu), \quad l = 0,1,2,\ldots,L-1;\ \mu \neq 0 \tag{2}$$

where $E[\cdot]$ is the statistical expectation and μ is the exponential decay rate of the diffuse power in each path. The probability density function (pdf) of the distributed Rayleigh random variables α_{il} is given by [5]

$$f_{\alpha_{il}}(x) = 2x/\psi_{il}\exp(-x^2/\psi_{il}), \quad x \geq 0 \tag{3}$$

where $\psi_{il} = E[\alpha_{il}^2]$, $i = 1,\ldots,D$, and $l = 0,\ldots, L-1$.

The receiving antenna is a linear array of M identical elements spaced d apart with $d = 0.5\lambda_c$ and λ_c is the wavelength of the carrier transmitted signal. Hence, the response vector of the antenna array is expressed as

$$\boldsymbol{a}(\theta) = \left[1\ e^{-j\pi sin\theta} \cdots e^{-j\pi(M-1)sin\theta}\right]^T \tag{4}$$

where θ is the direction of arrival (DOA) angle of the signal and T denotes transpose. LMS is an adaptive array antenna algorithm which would adapt iteratively its weight vector to any array response vector. The received signal consists of the signal from the first user, MAIs from the others, and an additive white Gaussian noise (AWGN) $n(t)$. Thus, the received signal at the m-th antenna element of the array is [38]

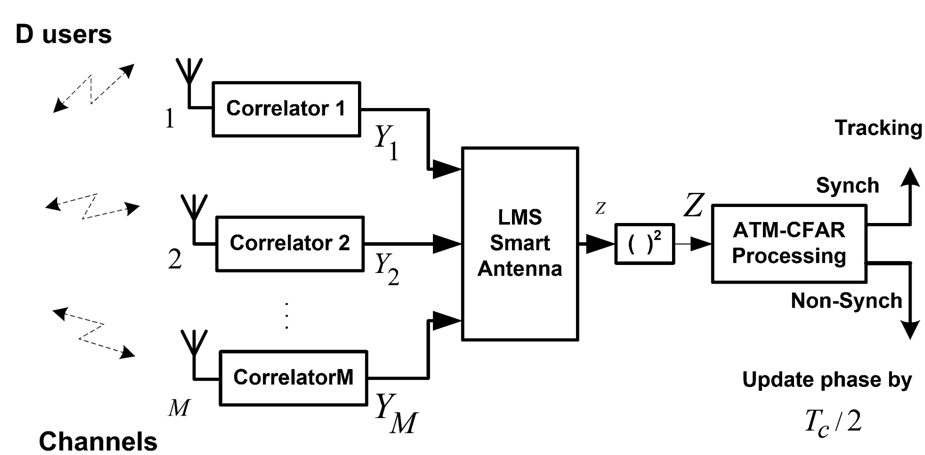

Fig. 1 Block diagram of the proposed communication system model

$$r_m(t) = \sqrt{2P_s}\left\{\sum_{l=0}^{L-1}\alpha_{1l}b_1(t-\tau_1-lT_c)c_1(t-\tau_1-lT_c)\right.$$
$$\left.\times\, cos(\omega_c t+\varphi_{1l})\exp(-j\pi(m-1)sin\theta_s)\right\}$$
$$+\left\{\sum_{i=2}^{D}\sqrt{2P_{I_{i-1}}}\sum_{l=0}^{L-1}\alpha_{il}b_i(t-\tau_i-lT_c)c_i(t-\tau_i-lT_c)\right.$$
$$\left.\times\, cos(\omega_c t+\varphi_{il})\ \exp(-j\pi(m-1)sin\theta_{i-1})\right\}+n_m(t);$$
$$m=1,2,\ldots,M \tag{5}$$

where P_s is the received signal power of the first user during initial synchronization, P_{Ii-1} is the received signal power of the interfering user $i-1$, τ_i is the relative time delay associated with the asynchronous communication channel model; $\varphi_{il} = \xi_i - \zeta_{il} - \omega_c(\tau_i + lT_c)$ is the phase in the demodulator of the receiver which $i = 2, 3,\ldots, D$, $l = 0, 1,\ldots, L-1$, T_c is the chip duration, θ_s is the DOA angle of the first user signal, θ_{i-1} is the DOA angle of the interfering user. In this paper we consider the pilot channel instead of pilot symbols and thus we set $b_i(t) = 1$.

3.2 Correlator

The correlator that follows the m-th antenna element is shown in Fig. 2. The equivalent baseband signal $r_m^{I'}(t)$ at the correlator can be written as follows

$$r_m^{I'}(t) = 2\sqrt{P_s}\left\{\sum_{l=0}^{L-1}\alpha_{1l}c_1(t-\tau_1-lT_c)cos(\omega_c t+\varphi_{1l})\right.$$
$$\left.\times\, cos(\omega_c t)\exp(-j\pi(m-1)\sin\theta_s)\right\}$$
$$+2\left\{\sum_{i=2}^{D}\sqrt{P_{I_{i-1}}}\sum_{l=0}^{L-1}\alpha_{il}c_i(t-\tau_i-lT_c)\right.$$
$$\left.\times\, cos(\omega_c t+\varphi_{il})cos(\omega_c t)\exp(-j\pi(m-1)sin\theta_{i-1})\right\}$$
$$+n_m(t); \tag{6}$$

The in-phase and quadrature phase (I–Q) components of the correlator are multiplied by the locally generated PN code $c(t - j_cT_c/2)$, $j_c = 0,1,\ldots,N_c$ (N_c represents the reference window size of the CFAR processor), and integrated over a dwell time interval $\tau_D = RT_c$ s, where R is the correlation length integer to yield respectively the I and Q branch components Y_m^I and Y_m^Q.

Then the output Y_m from each branch of the correlator gives the first user signal component, the MAI, and the AWGN, which can be expressed as

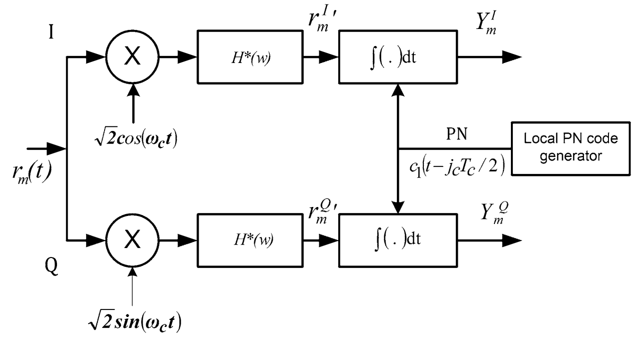

Fig. 2 Correlator consists of in-phase (I) and quadrature-phase (Q) components

$$Y_m = \left\{\sum_{l=0}^{L-1}\left(Y_{Sl}^I + jY_{Sl}^Q\right)\exp(-j\pi(m-1)sin\theta_s)\right\}$$
$$+\left\{\sum_{i=2}^{D}\sum_{l=0}^{L-1}\left(Y_{MAI\,il}^I + jY_{MAI\,il}^Q\right)\right. \tag{7}$$
$$\left.\times\,\exp(-j\pi(m-1)sin\theta_{i-1})\right\} + n_m$$

where $Y_{Sl}^I + jY_{Sl}^Q$ denotes I–Q component of the first user, $Y_{MAIil}^I + jY_{MAIil}^Q$ denotes I–Q component of the MAI, and $n_m(t) = N_m^I(t) + jN_m^Q(t)$ denotes the thermal noise. The in-phase signal component in (7) due to the first user is given by [8],

$$Y_{Sl}^I = \sqrt{P_S}\alpha_{1l}cos(\varphi_{1l})\left[\Delta_1R_p(j_c,N+1)+(T_c-\Delta_1)R_p(j_c,N)\right]$$
$$=\sqrt{P_S}R_{Sl}^I \tag{8}$$

where

$$R_{Sl}^I = \alpha_{1l}cos(\varphi_{1l})\left[\Delta_1R_p(j_c,N+1)+(T_c-\Delta_1)R_p(j_c,N)\right] \tag{9}$$

where Δ_1 is a random variable uniformly distributed in [0, T_c] and $R_p(j_c, N)$ is the code partial autocorrelation function of the first user. The quadrature phase signal component of the first user can be obtained by replacing $cos(\varphi_{il})$ with $-sin(\varphi_{il})$ in (8). The in-phase MAI term can be defined as

$$Y_{MAIil}^I = \sqrt{P_{I_{i-1}}}\alpha_{il}cos(\varphi_{il})[\Delta_iR_p^{(i)}(j_c,N+1)$$
$$+(T_c-\Delta_i)R_p^{(i)}(j_c,N)] \tag{10}$$
$$=\sqrt{P_{I_{i-1}}}R_{MAIil}^I$$

where

$$R_{MAIil}^I = \alpha_{il}cos(\varphi_{il})\left[\Delta_lR_p^{(i)}(j_c,N+1)+(T_c-\Delta_l)R_p^{(i)}(j_c,N)\right] \tag{11}$$

where $R_p^{(i)}(j_c,N)$ is the code partial cross-correlation between the received sequence of the $i-1$-th user and the locally generated sequence. The R^{I}_{MAIil} decreases the power of the interfering signal that comes out the correlator, which is affected by factor of $R_p^{(i)}(j_c,N)$. The quadrature phase signal term of MAIs can be obtained by replacing $cos(\varphi_{il})$ with $-sin(\varphi_{il})$ in (10); and the noise term is determined by

$$N_m^I = \int_0^{RT_c} n_m^I c_1(t - jT_c/2)\sqrt{2}cos(\omega_c t)dt \qquad (12)$$

The quadrature phase of the noise term is defined by replacing $cos(\varphi_{il})$ by $sin(\varphi_{il})$.

3.3 Smart antenna

Smart antenna in the proposed system performs adaptive beamforming by using the LMS algorithm by directing the main array pattern towards the preferred source signal and creating nulls in the directions of the interfering signals. The LMS algorithm computes iteratively the optimum beamforming weight vector with minimum square errors (MSE) between the desired signal value and the LMS processor output. We select the LMS algorithm because of its benefits such as simple, ease of implementation, good accuracy, and good convergence properties. The LMS algorithm has fewer of computational and easier for implementation compared to several algorithms; i.e., RLS and SMI. It also has accuracy as good as RLS algorithm. The input of the LMS processor comes from the output Y_m of M branches of the correlator which can be defined as follows

$$\boldsymbol{Y} = [Y_1\ Y_2 \cdots Y_M]^T \qquad (13)$$

The inputs of the LMS processor in (7) and (13) can be expressed as follows

$$\begin{aligned}\boldsymbol{Y} &= \boldsymbol{Y}_S^{IQ} + \boldsymbol{Y}_{MAI}^{IQ} + \boldsymbol{n}^{IQ} \\ &= \sum_{l=0}^{L-1} \boldsymbol{a}_{sl}(\theta_{sl})Y_S^{IQ} + \sum_{i=2}^{D}\sum_{l=0}^{L-1} \boldsymbol{a}_{i-1l}(\theta_{i-1l})Y_{MAI}^{IQ} + \boldsymbol{n}^{IQ}\end{aligned} \qquad (14)$$

where $\boldsymbol{a}_{sl}(\cdot)$ is the array steering vector of antenna to the first user or its replicates, $\boldsymbol{a}_{i-1l}(\cdot)$ is the array steering vector of antenna to the interfering user or the replicates, $Y_S^{IQ} = (Y_{Sl}^I + jY_{Sl}^Q)$, $Y_{MAI}^{IQ} = \left(Y_{MAIi-1l}^I + jY_{MAIi-1l}^Q\right)$, and $\boldsymbol{n}^{IQ} = [n_1^{IQ}\ n_2^{IQ}\ \cdots n_M^{IQ}]^T$. The LMS processor incorporates an iterative procedure that makes successive corrections to the weight vector

$$\boldsymbol{w}(n_c) = [w_1(n_c)\ w_2(n_c)\ \cdots\ w_M(n_c)]^T \qquad (15)$$

where n_c is a number of iterations until convergence is reached. Once the minimum MSE is attained we claim that the weight vector in (15) is optimum, which should increase the first user signal to the interference signal ratio (SIR). In other words, it keeps the signal power of the first user as the desired signal and reduces the MAI signal effect. Furthermore, this optimum weight vector is used to generate a spatial correlation output given by

$$z = \boldsymbol{w}_{opt}^{\boldsymbol{H}}\boldsymbol{Y} \qquad (16)$$

Substituting the input of the LMS processor in (14) into (16), we obtain z as follows

$$z = \boldsymbol{w}_{opt}^{\boldsymbol{H}}\left\{\sum_{l=0}^{L-1}\boldsymbol{a}_{sl}(\theta_{sl})Y_S^{IQ} + \sum_{i=2}^{D}\sum_{l=0}^{L-1}\boldsymbol{a}_{i-1l}(\theta_{i-1})Y_{MAI}^{IQ} + \boldsymbol{n}^{IQ}\right\} \qquad (17)$$

The output z in (17) shows the iterative procedure of the LMS processor weights of the first user signal, the MAI signals, and the AWGN. The weight affects the ratio of the signal power of interfering user $i-1$ to the first user signal after the LMS processor, which is β_{i-1}, $i = 2,\ldots, D$, while β_{i-1} is defined as

$$\beta_{i-1l} = \left\{\boldsymbol{w}_{opt}^{\boldsymbol{H}}\boldsymbol{a}_{i-1l}(\theta_{i-1l})Y_{i-1l}^{IQ}\right\}/\left\{\boldsymbol{w}_{opt}^{\boldsymbol{H}}\boldsymbol{a}_{s0}(\theta_{s0})Y_{S0}^{IQ}\right\} \qquad (18)$$

$\boldsymbol{a}_{s0}$ (θ_{s0}) is the array steering vector of antenna to the first user, $i = 2,\ldots, D$, and $l = 1, 2,\ldots,L-1$. Recall that the weighting of the LMS processor increases the signals to interference ratio (SIR) while the value of β_{i-1l} is decreased, which means the LMS decreases the interfering signal effect. Given the Gaussian nature of z^I and z^Q, the variable $Z = |z|^2$ follows a noncentral Chi square distribution law with two degrees of freedom [5]. Statistically, the pdf of Z given the amplitude of first user path α_{1l} corresponding to the l-th resolvable path can be written as

$$f_{Z|\alpha_{1l}}\left(z|\alpha_{1l},H_1^l\right) = \frac{1}{2\sigma_0^2 M_w}\exp\left(-\frac{\lambda^2 M_w^2 + z}{2\sigma_0^2 M_w}\right)I_0\left(\frac{\sqrt{\lambda^2 z}}{\sigma_0^2}\right), \quad z \geq 0 \qquad (19)$$

λ^2 is the normalized noncentral parameter given by $\lambda^2 = 9/16\alpha_{1l}^2$ [39]. $M_w = \boldsymbol{w}^H\boldsymbol{a}_{s0}(\theta_{s0})M$ is the LMS element weighting factor, σ_0^2 is the variance, and $I_0(\cdot)$ is the zeroth order modified Bessel function of the first kind. σ_0^2 is a representation of the background noise resulting from three signals, which are the self-interference from the nonaligned paths σ_S^2, the MAI caused by the interfering users σ_M^2, and thermal noises generated by the antenna array σ_N^2 as defined in [8] and given by

$$\sigma_S^2 = \psi_{1l}/(3R) \qquad (20)$$

$$\sigma_M^2 = \beta_{i-1lave}\psi_{i-1lave}/(3R) \qquad (21)$$

$$\sigma_N^2 = 1/(2RS_c) \qquad (22)$$

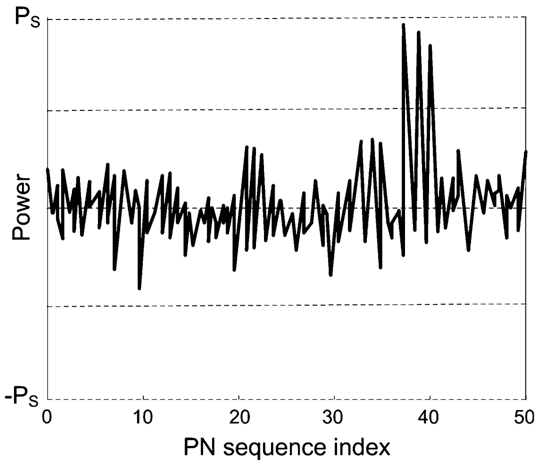

Fig. 3 Energy profile of the ATM-CFAR samples

$\beta_{i-1lave}$ denotes the average value of β_{i-1l} s, $\psi_{i-1lave}$ denotes the average value of ψ_{i-1l} s, and S_c denotes *SNR/chip* given by

$$S_c = T_c P_s / N_0 \tag{23}$$

The pdf of the decision variable Z under the aligned hypothesis corresponding to the l-th resolvable path is then obtained, after using Bayes theorem and doing some mathematical manipulations, to be

$$f_Z\left(z|H_1^l\right) = \frac{1}{2\sigma_0^2\left(M_w + M_w^2 v\right)} \exp\left(-\frac{z}{2\sigma_0^2\left(M_w + M_w^2 v\right)}\right), \quad z \geq 0 \tag{24}$$

where $v = 9\psi_{il}/(32\sigma_0^2)$. The pdf of decision variable Z under the nonaligned hypothesis is obtained from (24) to be

$$f_Z(z|H_0) = \frac{1}{2\sigma_0^2 M_w} \exp\left(-\frac{z}{2\sigma_0^2 M_w}\right), \quad z \geq 0 \tag{25}$$

3.4 Automatic trimmed mean (ATM) CFAR

In a multipath fading environment, the transmitted signal is usually reflected by a variety of buildings or terrains. The signals of the first user and other user signals are with a time delay. The multipath delay introduces a high partial autocorrelation between the sequence of the first user and the locally generated PN code sequence. In addition, there are partial cross-correlations between the locally generated sequence and the other users (MAIs). Hence, the output from the LMS processor consists of the multipath signals of the first user with high correlation value and noises with correlation values not significant. The environment and the process which the signal undergoes are:

1. The fading effect on each path as described in (2),
2. The autocorrelation value through the correlator as defined in (8), and
3. The weighting process by the LMS processor as described in (17) affects the value of multipath signals.

We consider the three parameters above as one value κ. The situation described above of the first user can be represented by Fig. 3 [40].These signals are the samples at the output of the LMS processor and the square operator. The distance between the multipath and noise samples is within thirty-two chips according to the PN code sequence index. The adaptive thresholding scheme used for maintaining the probability of false alarm constant during the code acquisition step in the spread spectrum communication considered is based on ATM-CFAR processing as shown in

Fig. 4 ATM-CFAR processor with fence outliers for defining multiplier values

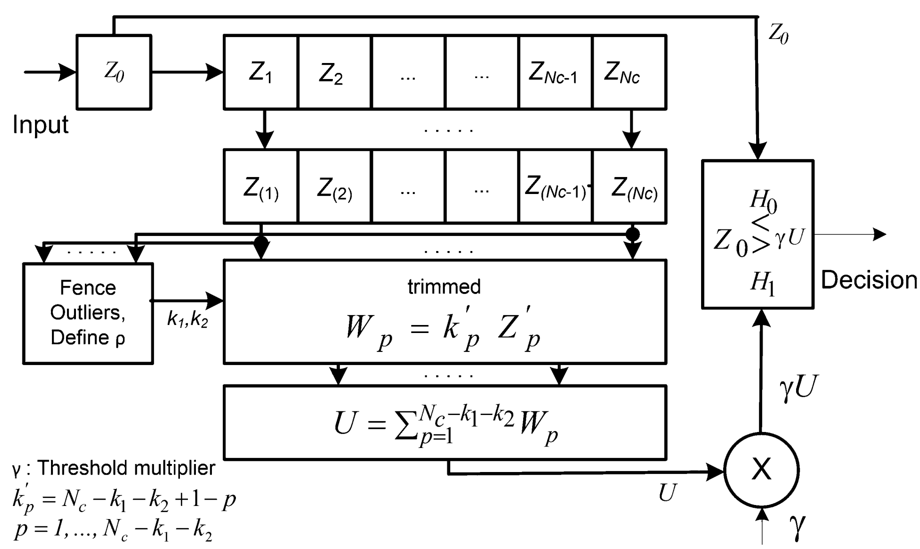

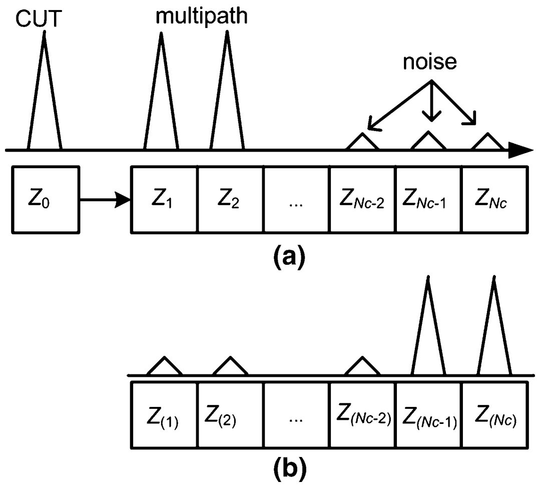

Fig. 5 Interference and noise in reference cell of ATM-CFAR processor

Fig. 4. It consists of three main parts which are the reference cells, the fences for the outliers, and the decision threshold. The output samples from the LMS processor are sent serially into a shift register of length N_c called reference window and containing the outputs of the previous N_c phases $Z_c, c = 1, 2, \ldots, N_c$. The contents of the reference cells are used according to some rule, which is adaptive trimmed mean in our case, as a statistic to represent the estimate of the background noise power level. The cell Z_0 represents the cell under test (CUT) of the current examined phase.

Due to the presence of multipath signals of the first user and noises, we assume r samples of interfering signals and $N_c - r$ samples with noise. The r interfering samples consist of multipath signals of the first user with high correlation values as shown in Fig. 5(a). These samples of the reference cells representing interfering signals plus noise are then arranged in ascending order according to their magnitudes $Z_{(1)}, Z_{(2)}, \ldots, Z_{(N_c)}$ as shown in Fig. 5(b). The ATM-CFAR processor censors k_1 cells from the lower end and k_2 cells from the upper end to eliminate the effect of the interfering signals. Hence, the fences as demarcation points of the outlier determiner are located at k_1 and $N_c - k_2$, which are obtained using the Boxplot technique. The interquartile range (IQR) measures a statistical dispersion which is equal to the difference between the third (Q_3) and the first (Q_1) quartiles. An outlier is the random variable that resides in the outlier region which are below of lower fence (LF) or above of upper fence (UF) given by

$$\begin{aligned} LF &= Q_1 - \rho(IQR) \\ UF &= Q_3 + \rho(IQR) \end{aligned} \tag{26}$$

where ρ is a multiplier value to determine the outlier fence. The process is summarized as follows:

Step 1 Define observation of sorted data $Z_{(1)}, Z_{(2)}, \ldots, Z_{(N_c)}$ from the reference cells. Then calculate the value of LF and UF.

Step 2 Define initial value of $k = 1$ as a cell index for data exploration of the reference cells.

Step 3 Determine a value of k_1, evaluate $LF \leq Z_{(k)}$ and increase the value of k. If the conditional upon $LF \leq Z_{(k)}$ is true, then repeat this step, otherwise set $k_1 = k$.

Step 4 To obtain a value of k_2, we evaluate $UF \geq Z_{(k)}$ and increase the value of k. If the conditional upon $UF \geq Z_{(k)}$ is true, then set $k_2 = N_c - k$, otherwise repeat the evaluation in this step.

Once we obtain k_1 and k_2 from the algorithm above, we censor k_1 cells from the lower end and k_2 from the upper end as in [41]. We perform a transformation of random variable on the remaining cells to obtain $W_p = k'_p Z'_p$, where $k'_p = N_c - k_1 - k_2 + 1 - p,\ p = 1, \ldots, N_c - k_1 - k_2$. The estimated noise level value U is obtained by calculating the arithmetic mean of the remaining non-censored cells $(N_c - k_1 - k_2)$ to yield

$$U = \sum_{p=1}^{N_c - k_1 - k_2} W_p \tag{27}$$

The estimated noise level value U is scaled by a threshold multiplier γ in order to achieve the designed false alarm probability. The probability of detection for the l-th resolvable path can be determined by

$$P_{dl} = \prod_{p=1}^{N_c - k_1 - k_2} \Omega_{W_p}\left(\frac{\gamma}{\eta(1 + M_w v)}\right) \tag{28}$$

where Ω_{W_p} is the moment generating function (mgf) of the random variables W_p's, $\eta = 2\sigma_0^2 M_w$. The individual mgf of W_p's are given by:

$$\begin{aligned} \Omega_{W_1}\left(\frac{\gamma}{\eta(1 + M_w v)}\right) &= q_1 \binom{N_c}{k_1} \sum_{b=0}^{k_1} (-1)^b \\ &\times \binom{k_1}{b} \frac{1}{\gamma/(1 + M_w v) + q_1 + q_1 b/(N_c - k_1)} \end{aligned} \tag{29}$$

$$\Omega_{W_p}\left(\frac{\gamma}{\eta(1+M_w v)}\right)\begin{cases} = \dfrac{q_p}{\gamma/(1+M_w v)+q_p}, & p=2,\ldots,N_c-r-k_1 \\ = \dfrac{q_p}{\gamma(1+M_w I)/(1+M_w v)+q_p}, & p=N_c-r-k_1+1,\ldots,N_c-k_1-k_2 \end{cases} \tag{30}$$

where $q_p=(N_c-k_1+1-p)/(N_c-k_1-k_2+1-p)$, q_1 is q_p with $p=1$, and $I=l\sigma_S^2/\sigma_N^2$.

The overall probability of detection P_d of the ATM CFAR processor is the expected value of the probability of detection for the l-th resolvable path P_{dl} with respect to the priori distribution. The probability of false alarm can be calculated theoretically by replacing $\gamma/(1+M_w v)$ with γ in (28) to obtain

$$P_f=\prod_{p=1}^{N_c-k_1-k_2}\Omega_{W_p}\left(\frac{\gamma}{\eta}\right) \tag{31}$$

The CUT Z_0 is then compared to the adaptive threshold γU to decide H_1^l or H_0. H_1^l means the sample Z exceeds the detection threshold γU and then tracking is performed. Otherwise, decide H_0 which means there is no acquisition.

4 Results and discussions

In this section, we investigate the detection performance and the multiplier value ρ to determine the demarcation points at the lower and upper trimming of the proposed communication system for various parameters. The design probability of false alarm is $P_{fa}=10^{-3}$. Figure 6 shows a comparison of P_d between the proposed system and the system in [3] [using Eq. (31)]. The received signal comes from the first user signal without multipath of the first user. The lower trim k_1 and upper trim k_2 are equal to zero. The correlation length integer of the dwell time interval is $R=128$, and the number of reference cells are $N_c=16$ and 32. The proposed system with a number of reference cells $N_c=16$ (dotted lines), lower trim $k_1=0$, and upper trim $k_2=0$, has slightly lower performance than the one in [3], but the same performance when $N_c=32$. We note that the detection probability increases as the number of reference cells N_c increases as expected. We observe, however, that the proposed system with smart antennas can detect signals with lower SNRs.

With $N_c=16$ and $M=1$ we have a probability of detection $P_d=0.9$ at an *SNR/chip* $=0$ dB, whereas with $N_c=16$ and $M=5$ we get the same P_d at a much lower *SNR/chip* $=-6$ dB. In other words, P_d increases as the number of antenna elements increases.

Figure 7 shows the simulated values of ρ using (26) against *SNR/chip* for several cell index values k's when the number of reference cells $N_c=32$, the number of multipath $L=3$, and the number of users $D=3$. $\rho_{\max}$ denotes

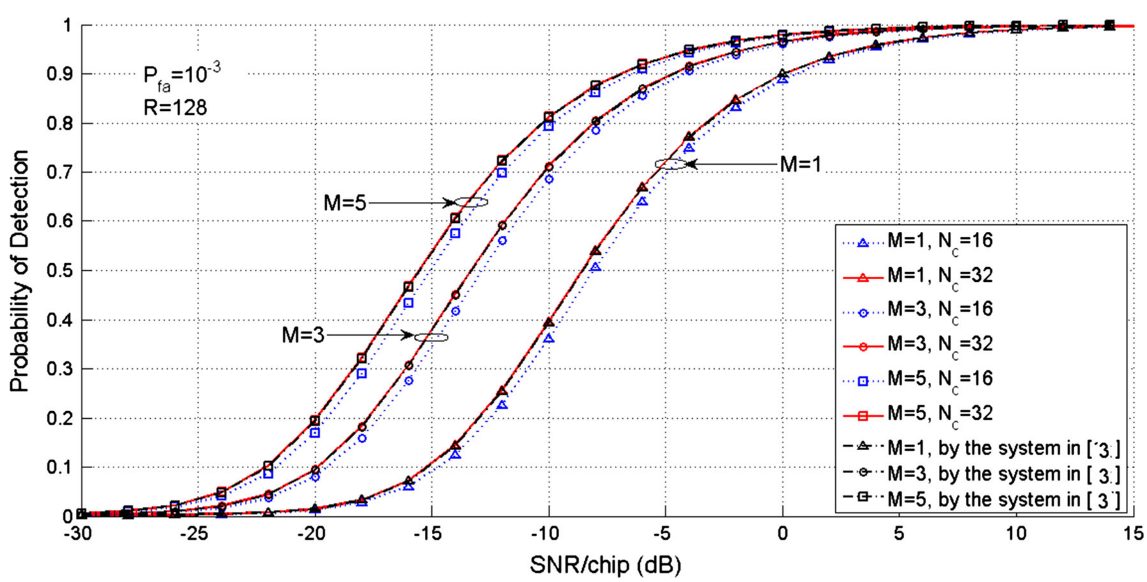

Fig. 6 Comparison of probabilities of detection between the proposed system and system in [3] with N_c and M as parameters; $P_{fa}=10^{-3}$, $R=128$

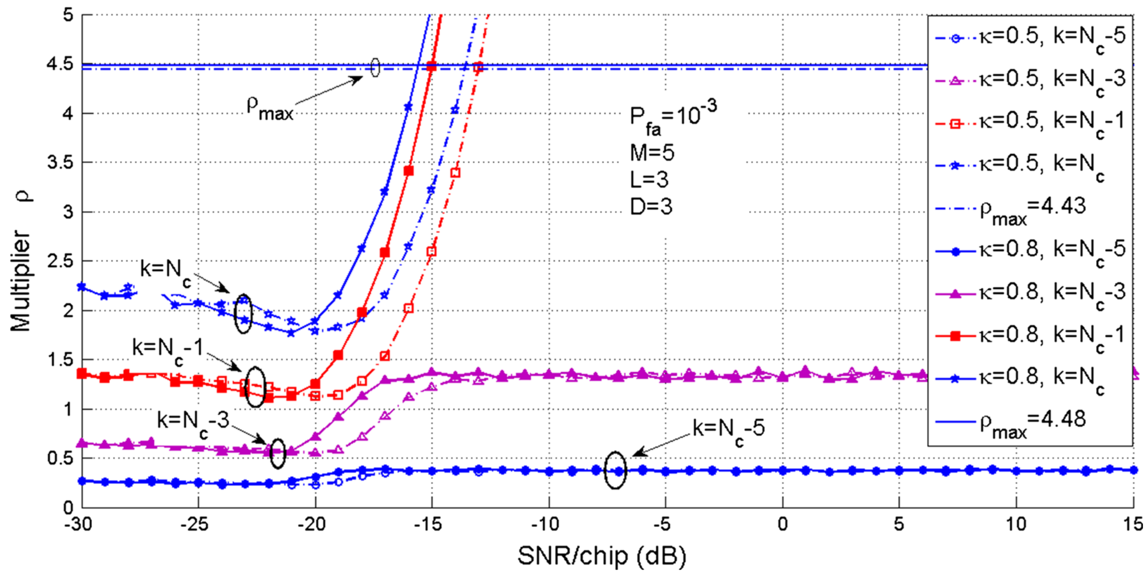

Fig. 7 Multiplier (ρ) values of the proposed system for varying κ and k; with $P_{fa} = 10^{-3}$, $M = 5$, $L = 3$, and $D = 3$

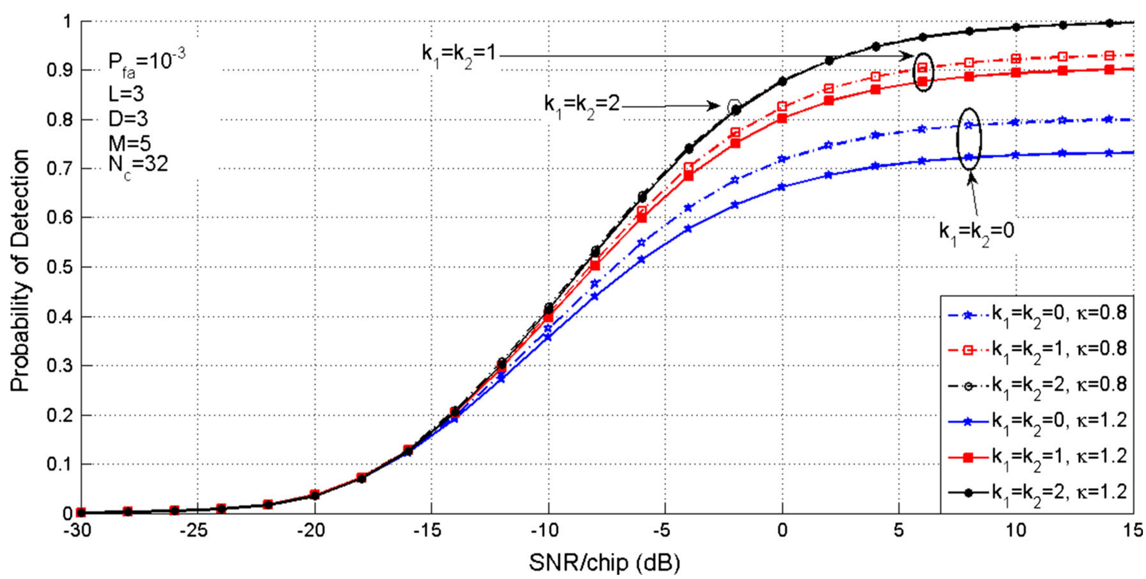

Fig. 8 Probabilities of detection of the system for varying κ, k_1 and k_2; with $P_{fa} = 10^{-3}$, $M = 5$, $L = 3$, $D = 3$, and $N_c = 32$

the maximum value which limits the fence at cell index value less than the number of the reference cells N_c. The value of ρ for a reference cell that does not contain interference will never reach $\rho_{\max}$, e.g., $\rho_{k=Nc-3}$. Based on the simulated results, we can obtain the appropriate ρ to determine the fences at k_1 and $N_c - k_2$ using the algorithm as explained above at Sect. 2. In [34], it is suggested that a ρ with values of 1.5 and 3.0 would not be appropriate for our system. We observe that the proposed system will censor cells that contain interference appropriately by using ρ less than the suggested values in [34].

In Fig. 8, we give the probability of detection P_d for $M = 5$ while varying κ, k_1 and k_2. We observe that the performance of the system decreases as κ increases but once apply the ATM CFAR processing as suggested P_d is seriously improved which emphasizes the robustness of the algorithm proposed. In Fig. 9 we observe that for $\kappa = 0.8$ while varying R, the performance of the system is significantly degraded by the presence of the interferences, that is there is no censoring ($k_1 = k_2 = 0$). At low *SNR/chip* the probability of detection increases as the correlation length integer R increases; e.g., with $k_1 = k_2 = 0$ and *SNR/chip* $= -10$ dB, the P_d of the system for $R = 128$ and $R = 256$ are 0.38 and 0.51, respectively.

In Fig. 10, we plot the probability of detection P_d for $\kappa = 1$, antenna elements $M = 1$ and $M = 5$ while varying

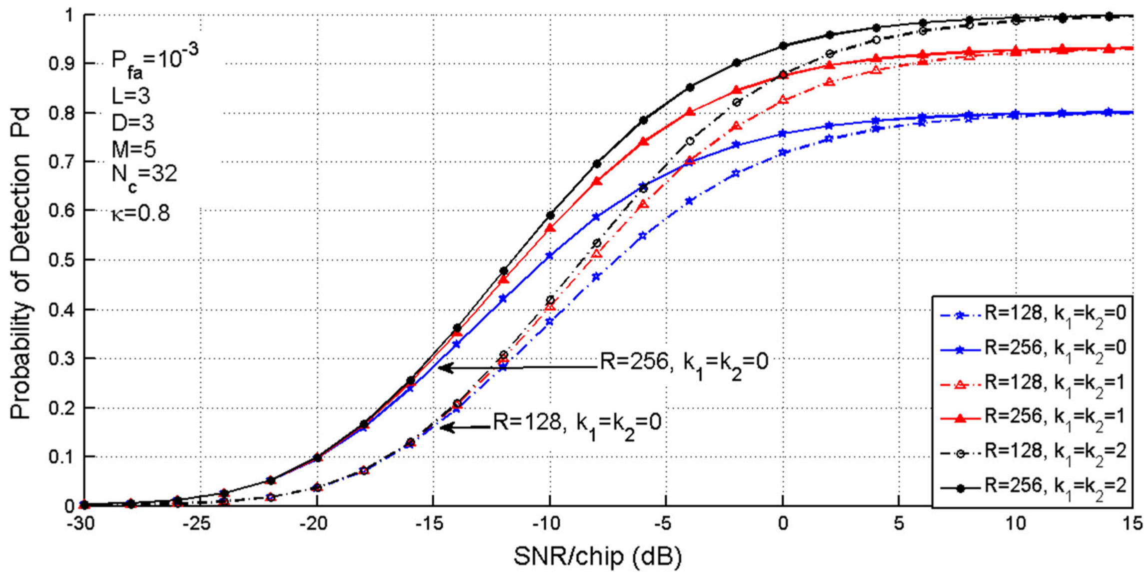

Fig. 9 Probabilities of detection of the system for varying R, k_1, and k_2; with $P_{fa} = 10^{-3}$, $M = 5$, $L = 3$, $D = 3$, $N_c = 32$ and $\kappa = 0.8$

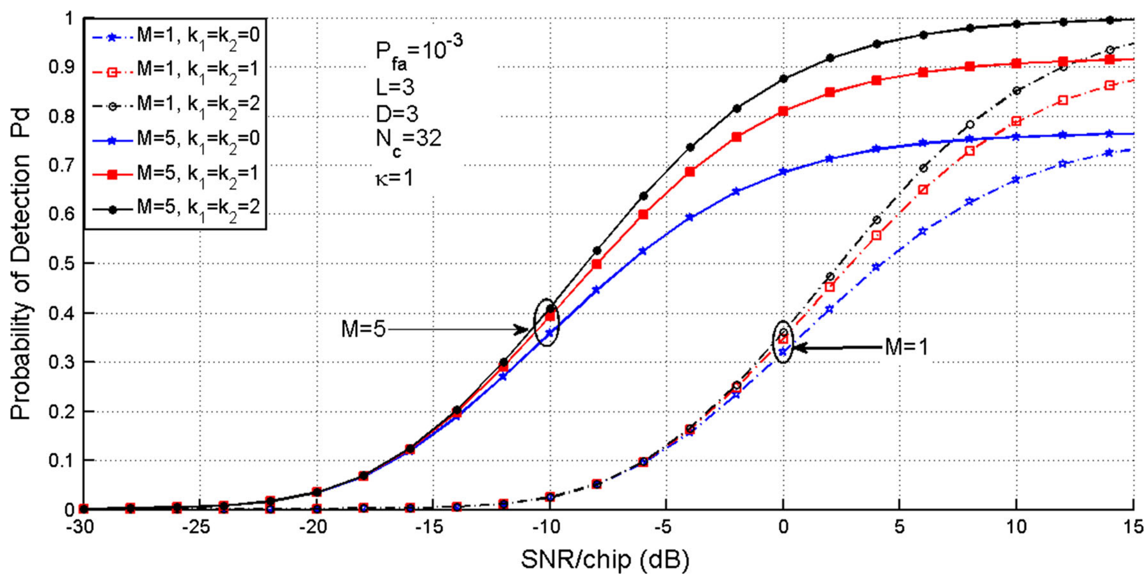

Fig. 10 Probabilities of detection of the system for varying M, k_1, and k_2; with $P_{fa} = 10^{-3}$, $M = 5$, $L = 3$, $D = 3$, $N_c = 32$ and $\kappa = 1$

the censoring points k_1, and k_2. The performance of the system increases as the number of antenna elements increases as expected.

We also observe that even without censoring the interferences, the detection performance of the system with $M = 5$ is better than that of the system with $M = 1$; e.g., with $k_1 = k_2 = 0$ and for $SNR/chip = 0$ dB, P_d of the proposed system with $M = 5$ and $M = 1$ are 0.69 and 0.32, respectively. The smart antenna allows an enhancement of 0.37 (115 %). With censoring and if $k_1 = k_2 = 2$, which is equal to the number of multipath considered, for an $SNR/chip = 0$ dB, P_d of the system for $M = 5$ and $M = 1$ are 0.88 and 0.36, respectively, which shows a significant enhancement of 0.52 (144 %). Hence, the proposed system shows robustness as the probability of detection is significantly improved.

5 Conclusion

In this paper, we have proposed a spread spectrum communication system using smart antennas and adaptive ATM-CFAR processing with fence outliers determiner, a robust algorithm based on rank order statistics, for direct sequence PN code acquisition. We developed expressions for the conditional probability density functions of the aligned and the nonaligned hypotheses using the LMS algorithm. The performance of the proposed system was studied in terms of simulated curves of the probability detection for several parameters. As expected, increasing number of reference cells in ATM-CFAR processing and the number of antenna elements enhanced the detection performance. In addition, by appropriately censoring the cells containing interferences, the performance of the systems is more robust compared to the system proposed in [3]. Recall that the performance of the system in [3] was only comparable to the proposed system with the conventional CA-CFAR processing. We also investigated values of ρ to determine the fences for proper identification of outliers. This approach of using a smart antenna with adaptive thresholding ATM-CFAR processing with an outlier determiner proved to be robust in combating MAI and multipath since the probability of detection improved significantly.

Acknowledgments This work was supported by the Research Centre of College of Computer and Information Sciences, King Saud University. The authors are grateful for this support.

References

1. Chryssomallis, M. (2000). Smart antennas. *IEEE Antennas Propag. Mag., 42*, 129–136.
2. Godara, L. C. (2004). *Smart antenna*. New York: CRC Press LLC.
3. Bing, W., & Kwon, H. M. (2003). PN code acquisition using smart antenna for spread-spectrum wireless communications. I. *IEEE Trans. Veh. Technol., 52*, 142–149.
4. Bing, W., & Kwon, H. M. (2003). PN code acquisition for DS-CDMA systems employing smart antennas. II. *IEEE Trans. Wireless Commun., 2*, 108–117.
5. Barkat, M. (2005). *Signal detection and estimation* (2nd ed.). Boston, MA: Artech House.
6. Sofwan, A., & Barkat, M. (2012). PN code acquisition using smart antennas and adaptive thresholding trimmed-mean CFAR processing for CDMA communication. In *Spring Congress on Engineering and Technology (S-CET)* (pp. 1–4).
7. Polydoros, A., & Weber, C. (1984). A unified approach to serial search spread-spectrum code acquisition—Part I: General theory. *IEEE Trans. Commun., 32*, 542–549.
8. Lie-Liang, Y., & Hanzo, L. (2001). Serial acquisition of DS-CDMA signals in multipath fading mobile channels. *IEEE Trans. Veh. Technol., 50*, 617–628.
9. Sourour, E. A., & Gupta, S. C. (1990). Direct-sequence spread-spectrum parallel acquisition in a fading mobile channel. *IEEE Trans. Commun., 38*, 992–998.
10. Rick, R. R., & Milstein, L. B. (1997). Parallel acquisition in mobile DS-CDMA systems. *IEEE Trans. Commun., 45*, 1466–1476.
11. Zhuang, W. (1996). Noncoherent hybrid parallel PN code acquisition for CDMA mobile communications. *IEEE Trans. Veh. Technol., 45*, 643–656.
12. Van Der Meer, A., & Liyana-Pathirana, R. (2003). Performance analysis of a hybrid acquisition system for DS spread spectrum. In *TENCON 2003 Conference on Convergent Technologies for Asia-Pacific Region* (Vol. 1, pp. 121–125).
13. Rick, R. R., & Milstein, L. B. (1997). Parallel acquisition of spread-spectrum signals with antenna diversity. *IEEE Trans. Commun., 45*, 903–905.
14. Oh-Soon, S., & Kwang Bok, L. (2003). Use of multiple antennas for DS/CDMA code acquisition. *IEEE Trans. Wireless Commun., 2*, 424–430.
15. Meng, W., Sun, S., Chen, H., & Li, J. (2013). Multi-user interference cancellation in complementary coded CDMA with diversity gain. In *IEEE Wireless Communications Letters* (Vol. PP, pp. 1–4).
16. Dodd, R., Schlegel, C., & Gaudet, V. (2013). DS-CDMA implementation with iterative multiple access interference cancellation. *IEEE Trans. Circuits Syst. I Regul. Pap., 60*, 222–231.
17. Al-fuhaidi, B. A., Hassan, H. E. A., Salah, M. M., & Alagooz, S. S. (2012). Parallel interference cancellation with different linear equalisation and rake receiver for the downlink MC-CDMA systems. *IET Commun., 6*, 2351–2360.
18. Zhang, X., Gao, X., & Wang, Z. (2009). Blind paralind multiuser detection for smart antenna CDMA system over multipath fading channel. *Prog. Electromagn. Res., 89*, 23–38.
19. Recioui, A., Bentarzi, H., Azrar, A., Dehmas, M., & Challal, M. (2009) Combating multiple access interference in wireless communication systems employing Smart Antennas. In *6th International Multi-Conference on Systems, Signals and Devices* (pp. 1–4).
20. Dau-Chyrh, C., & Cheng-Nan, H. (2012). Smart antennas for advanced communication systems. *Proc. IEEE, 100*, 2233–2249.
21. Finn, H. M., & Johnson, R. S. (1968). Adaptive detection mode with threshold control as a function of spatially sampled clutter-level estimates. *RCA Rev., 29*, 414–464.
22. Habib, M. A., Barkat, M., Aissa, B., & Denidni, T. A. (2008). CA-CFAR detection performance of radar targets embedded in "non centered Chi-2 gamma" clutter. *Prog. Electromagn. Res., 88*, 135–148.
23. Rohling, H. (1983) Radar CFAR thresholding in clutter and multiple target situations. In *IEEE Transactions on Aerospace and Electronic Systems* (Vol. AES-19, pp. 608–621).
24. Himonas, S. D., & Barkat, M. (1992). Automatic censored CFAR detection for nonhomogeneous environments. *IEEE Trans. Aerosp. Electron. Syst., 28*, 286–304.
25. Cho, C. M., & Barkat, M. (1993). Moving ordered statistics CFAR detection for nonhomogeneous backgrounds. *IEE Proc. F Radar and Signal Process., 140*, 284–290.
26. Oh, H.-S., & Han, D.-S. (2005). An adaptive double-dwell PN code acquisition system in DS-CDMA communications. *Sig. Process., 85*, 2327–2337.
27. Chang-Joo, K., Dong-Doo, L., Tae-Won, H., Hyuck-Jae, L., & Hwang-Soo, L. (1998). Adaptive hybrid acquisition of PN sequences for DS/SS communications. *Electron. Lett., 34*, 939–940.
28. Benkrinah, S., & Barkat, M. (2005) An adaptive acquisition using order statistic CFAR in DS-CDMA serial search for a multipath Rayleigh fading channel. In *The Third IEEE International Conference on Systems, Signals and Devices*, Tunisia.
29. Bekhakhecha, R., Barkat, M., & Alshebeili, S. (2006) Adaptive acquisition of a PN code using OS-CFAR detection and antenna diversity for a multipath Rayleigh fading channel. In International *Conference on Computer and Communication Engineering*, Malaysia.
30. Berbra, K., Barkat, M., & Anou, A. (2014). PN code acquisition using smart antenna and adaptive thresholding CFAR based on ordered data variability for CDMA communications. *Prog. Electromagn. Res. B, 57*, 139–155.
31. Lehtomaki, J. J., Vartiainen, J., Juntti, M., & Saarnisaari, H. (2007). CFAR outlier detection with forward methods. *IEEE Trans. Signal Process., 55*, 4702–4706.

32. Tuckey, J. W. (1977). *Exploratory data analysis* (1st ed.). Boston, MA: Addison-Wesley.
33. Barnett, V., & Lewis, T. (1994). *Outliers in statistical data* (3rd ed.). New York: Wiley.
34. Hoaglin, D. C., Iglewicz, B., & Tuckey, J. W. (1986). Performance of some resistant rules for outlier labeling. *J. Am. Stat. Assoc., 81*, 991–999.
35. Sim, C. H., Gan, F. F., & Chang, T. C. (2005). Outlier labeling with boxplot procedures. *J. Am. Stat. Assoc., 100*, 642–652.
36. Proakis, J. G. (2001). *Digital communications* (4th ed.). New York: McGraw-Hill Book Inc.
37. Rick, R. R., & Milstein, L. B. (1998). Optimal decision strategies for acquisition of spread-spectrum signals in frequency-selective fading channels. *IEEE Trans. Commun., 46*, 686–694.
38. Song, Y. S., Kwon, H. M., & Min, B. J. (2001). Computationally efficient smart antennas for CDMA wireless communications. *IEEE Trans. Veh. Technol., 50*, 1613–1628.
39. Yang, L. L., & Simsa, J. (2000). Performance evaluation of spread-spectrum code acquisition using four-state Markov process. *IEEE Proc. Commun., 147*, 231–238.
40. Chang-Joo, K., Tae-Won, H., Hyuck-Jae, L., & Hwang-Soo, L. (1997). Acquisition of PN code with adaptive threshold for DS/SS communications. *Electron. Lett., 33*, 1352–1354.
41. Gandhi, P. P., & Kassam, S. A. (1988). Analysis of CFAR processors in nonhomogeneous background. *IEEE Trans. Aerosp. Electron. Syst., 24*, 427–445.

Aghus Sofwan received the Bachelor's and Master's degree in Electrical Engineering from Diponegoro University, and Gadjah Mada University in Indonesia, in 1995 and 2002, respectively. He is currently pursuing the Ph.D. degree in Computer Engineering at King Saud University, KSA. His research interests include signal detection, array signal processing techniques, and cognitive radio wireless network.

Mourad Barkat IEEE Fellow, got his Bachelor's with high honors (magna Cum Laude), Master's and Ph.D. from Syracuse University, New York in 1981, 1983, and 1987, respectively. He has over 30 years of international experience in teaching and research at Syracuse University, State University of New York (SUNY) at Stony Brook, University of Constantine, Algeria, American University of Sharjah, UAE, and King Saud University, KSA and Valencia College, USA. He is also an official ABET Program Evaluator for ABET Program Accreditation. He has authored and co-authored over 150 journal/conference papers, and he is the author of the book "Signal Detection and Estimation" Second Edition, Artech House: Massachusetts, 2007, a textbook well adopted by graduate schools worldwide. He is member of Tau Beta Pi and Eta Kappa Nu engineering honor societies and a recipient to many prestigious international awards.

Salman A. AlQahtani is currently an associate professor at the Department of Computer Engineering, College of Computer and Information Sciences, King Saud University, Riyadh, Saudi Arabia. He serves also as a senior consultant in computer communications, integrated solutions and digital forensics for few development companies and government sectors in Saudi Arabia. His main research activities are in Radio Resource Management (RRM) for wireless and cellular networks (3G, 4G, Wimax, LTE, LTE-Advanced, Femtocell, Cognitive radio,…) with focus on Call Admission Control (CAC), Packet Scheduling, radio resource sharing and Quality-of-Service (QoS) guarantees for data services. In addition, his interests also include performance evaluation of packet switched network, system model and simulations and integration of heterogeneous wireless networks. Finally, my interests also extend to the area of digital forensics.